J Mater Sci (2008) 43:1026–1032
DOI 10.1007/s10853-007-2242-1

# Embrittlement of polypropylene fibre during thermal oxidation

**Bruno Fayolle · Emmanuel Richaud · Jacques Verdu · Fabienne Farcas**

Received: 26 June 2007 / Accepted: 18 October 2007 / Published online: 15 November 2007


**Abstract** Polypropylene (PP) fibres for geotextile applications were oxidized under two exposure conditions: 110 °C in air under atmospheric pressure and 80 °C under pure oxygen at 5 MPa pressure corresponding to two distinct ISO standards. Fibre ageing has been monitored by rheometric molar mass, WAXS and tensile measurements. The results put in evidence the existence of predominant chain scission, chemicryrallization and embrittlement, the latter occurring at a structural state ($M_W = 130$ kg mol$^{-1}$, crystallinity ratio 80%) almost independent of exposure conditions. The relationships between all processes are discussed.

## Introduction

Isotactic polypropylene (PP) is especially interesting for geotextile applications, owing to its good mechanical properties, insensitivity to humid ageing, ease of processing and relatively low cost. Its durability can be however limited, in certain circumstances, by its relatively high sensitivity to radical chain oxidation. The latter induces random chain scission process in the amorphous phase and deep embrittlement occurs at low conversions of this degradation process [1].

B. Fayolle (✉) · E. Richaud · J. Verdu
Laboratoire d'Ingénierie des Matériaux, UMR 8006, ENSAM, 151 Bd de l'Hôpital, Paris 75013, France
e-mail: bruno.fayolle@paris.ensam.fr

F. Farcas
Laboratoire Central des Ponts et Chaussées, Service Physico-Chimie des Matériaux, 58 Bd Lefebvre, Paris 75015, France

This process has been investigated in the case of quasi-isotropic PP samples, for instance, films or moulded plaques as well in the case of thermooxidation [2] as in the case of photooxidation [3] or radiochemical oxidation [4]. A common feature of these ageing processes is the suddenness of the ductile to brittle transition indicating presumably that a critical state has been reached.

The existence of a critical molar mass $M_C'$ separating ductile (tough) and brittle regimes is now well documented in the case of amorphous polymers [5–7]: it has been shown that embrittlement is clearly related with the destruction of the entanglement network. In this case, $M_C'$ is relatively sharply linked to the entanglement molar mass $M_e$ typically $2M_e < M_C' < 10M_e$.

More recent studies showed, however, that semi-crystalline polymers having their amorphous phase in rubbery state (PE, PP, PTFE, POM) differ significantly from amorphous ones since in their case $M_C' > 10M_e$ [8–10]. This means that embrittlement occurs far before the entanglement network in amorphous phase is significantly damaged. It was recently hypothesized that, in this case, embrittlement is due to morphological changes [8]. As a matter of fact, it is well known for a long time that the polymers under consideration undergo "chemicrystallisation" induced by chain scission in their amorphous phase [11]: chain segments initially "trapped" in the entanglement network are liberated by a chain scission and can move towards a lamella to enter the crystalline phase. On the other hand, it is also well known that above a certain crystallinity ratio, polymers display always a brittle behaviour under tension [12]. Systematic investigations on polyethylene samples differing by their molar mass distribution or thermal treatment showed that the key factor could be the interlamellar distance, e.g. the thickness $l_a$ of the amorphous layer separating two lamellae [12].

All the above-described features are now well established for quasi-isotropic samples. However, the conclusions can be applied generally to highly oriented samples displaying very different morphologies. The aim of this article is to try to answer this question from an investigation on thermal oxidation of PP geotextile fibres. It has been chosen to study thermal ageing at 110 °C under atmospheric pressure, e.g. far below melting point (165 °C for the fibres under study) and at 80 °C under pure oxygen at 5 MPa. It has been shown that exposure in these latter conditions substantially increases the oxidation rate [13, 14].

## Experimental

### Material and processing conditions

Experiments were performed on polypropylene fibres provided by Tencate. PP fibres contained two types of stabilizers: phenol and phosphite. Initial weight average molar mass of the isotactic polypropylene was estimated at 170 kg $mol^{-1}$ and polydispersity index close to 2.5 by rheological measurements (see below). The polypropylene fibres were extruded at 240 °C, they were molten spun under pressure (1.4) with an extrusion rate of 250 m $s^{-1}$. The final fibre diameter is close to 30 μm.

### Exposure conditions

Exposure conditions have been chosen according to two European standards "Geotextiles and geotextile-related products-screening test method for determining the resistance to oxidation". For the first one named ENV ISO 13438 1998, the resistance to oxidation is tested by carrying out an oven-ageing experiment at 110 °C. For the second one named ENV ISO 13438 2002, the resistance to oxidation is tested by carrying out ageing experiment at 80 °C under 5 MPa of oxygen pressure. Oxidations under enhanced oxygen pressure were performed in autoclave devices.

## Characterization

### Molar mass measurements

The zero shear viscosity $\eta_0$ was measured in dynamic oscillatory mode with a Rheometrics Scientific ARES rheometer using parallel plate geometry (plate diameter 25 mm and gap 0.5 mm). The tests were performed under nitrogen at 190 °C with frequencies ranging between 0.05 and 100 rad $s^{-1}$ and with a maximum strain amplitude optimized to measure reliable torque values in the Newtonian domain. In order to avoid secondary thermolysis in the rheometer cell, the films were previously treated with sulphur dioxide in order to decompose hydroperoxides. After a 24 h treatment at ambient temperature, no subsequent thermal degradation was observed during rheometric measurements. Weight average molecular weight was determined at 210 °C according to: $\eta_0 = KM_w^{3.4}$, where $\eta_0$ is in Pa s and M in g $mol^{-1}$. The constant $K$ value of $1.072 \times 10^{-15}$ was determined by SEC and viscosity measurements performed on the virgin polymer. The molar mass distribution was determined from the viscoelastic spectrum using Mead's model [15].

### X-ray diffraction

Wide angle X-ray diffraction experiments were conducted in a Philips X'pert MRD diffractometer employing Cu Kα radiation at 40 mA and 40 kV. Since the fibre diameter is close to 30 μm, the fibres were winded into a ball in order to obtain a scan (20–47°) with a good resolution. For a given ball, measurements were performed at three different orientations (0°, 45°, 90°) in order to check isotropic character of the ball. Crystallinity ratio was estimated by deconvoluting diffractogram and determining areas corresponding to crystalline peaks and amorphous halo.

### Scanning electron microscopy (SEM)

The observations were made on gold-coated specimens using a Philips XL30 SEM with an electron acceleration voltage of 10 kV. The morphological changes were investigated by observing the specimens under various magnifications.

### Mechanical properties

The mechanical tests were carried out on a tensile testing machine INSTRON 4502 at 23 °C. Tensile measurements were performed at a constant crosshead displacement rate at 50 mm $min^{-1}$ and using a 100 N cell. Pneumatic grips were used to avoid fibre sliding. Only ultimate engineering strains are reported here; no corrections were made for thickness and width changes induced by necking.

## Results

### Structural modifications

Weight average molar mass ($M_W$) changes are reported in Fig. 1. For both exposure conditions, $M_W$ decreases rapidly

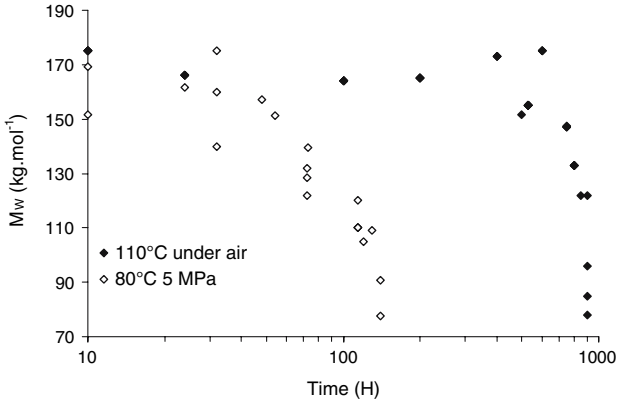


**Fig. 1** Weight average molar mass ($M_W$) as function of time of exposure: at 110 °C under air (♦) and at 80 °C under 5 MPa of oxygen (◇)

at the end of an induction period of which the duration is close to 500 h at 110°C in air and about ten times shorter at 80 °C under high oxygen pressure. It is thus confirmed that chain scission predominates in PP oxidation [1] and that oxidation rate is an increasing function of oxygen pressure [14]. The fact that polydispersity index remains constant and close to 2 indicates that chain scission is a random process and that crosslinking is negligible [16]. So, it can be written:

$$s(t) = 2\left(\frac{1}{M_W(t)} - \frac{1}{M_{W0}}\right)$$

$s$ being the number of chain scissions per mass unit.

WAXS diffractograms of initial fibre balls at different orientations are shown in Fig. 2. They appear to be practically independent of sample orientation, so that fibre balls can be considered isotropic and their diffractogram can be used for determination of the crystallinity ratio. The diffractograms are characteristic of the monoclinic a crystal structure, with peaks corresponding to (110), (040), (130) and (111) planes.

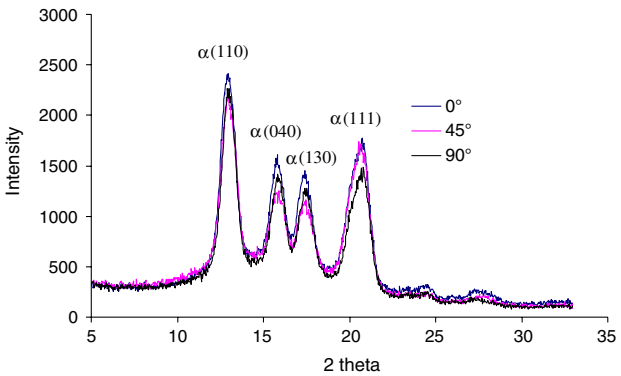


**Fig. 2** X-ray diffractometer scans of PP fibre at different orientation angles

The crystallinity ratio $X_C$ was plotted against exposure time for both exposure conditions in Fig. 3. $X_C$ increases slowly at the beginning of exposure and more rapidly after the end of induction period. Since no change of molar mass occurs during the induction period, it is reasonable to suppose that the corresponding increase in crystallinity is due to some annealing effect. In this case, the rapid increase of $X_C$ after the end of induction period must be attributed to another cause. This first explanation which comes in mind is a chain scission induced chemicrystallization [11].

At 110 °C in air, both mechanisms are well decoupled: $X_C$ increases until a value of ~70% as a result of annealing in the first ~100 h of exposure. Then, it reaches an asymptotic value corresponding to the "equilibrium" crystallinity value for the initial molar mass distribution under investigation. After the end of the induction period, $X_C$ increases abruptly from about 70% to more than 90% in less than 300 h. The increase coincides with the decrease of $M_W$. At 80 °C, both mechanisms are less clearly decoupled, presumably because the end of induction period occurs before the "equilibrium" crystallinity was reached.

## Embrittlement process

A typical (nominal) stress–strain curve for a virgin fibre is shown in Fig. 4. Tensile tests have been performed for samples aged in both above-defined conditions. The stress at break ($\sigma_R$) and strain at break ($\varepsilon_R$) have been recorded and the corresponding points were also plotted in Fig. 4 for samples exposed at 110 °C in air. The rupture envelope $\sigma_R = f(\varepsilon_R)$ is very close to the initial tensile curve, that seems to be a very general property of low temperature ageing processes in which chain scission predominates [2].

In such cases, strain at break is a pertinent criterion to monitor embrittlement process as shown, for instance, in the case of radiochemical initiated oxidation. Basically, there are only two possible causes of embrittlement: a

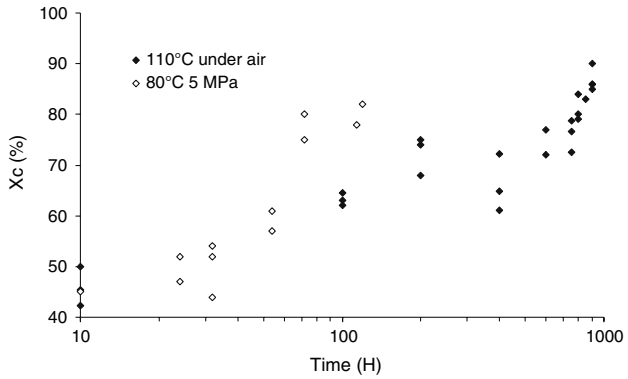


**Fig. 3** Crystallinity ratio ($X_C$) as function of time of exposure: at 110 °C under air (♦) and at 80 °C under 5 MPa of oxygen (◇)

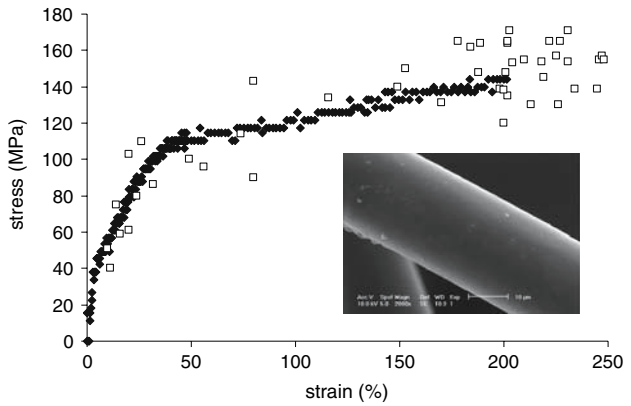


**Fig. 4** Stress–strain curve for initial fibre (♦) and stress–strain at break points (□) during exposure at 110 °C in air

decrease in toughness or a flaw build-up. In order to check the latter hypothesis, SEM observations of brittle fibres (i.e. with ageing times longer than the induction period) have been performed (Fig. 4). No microcracks were observed at the fibre surface at the micrometric scale. Applying the well-known Griffith law for crack initiation and considering the order of magnitude for polymer toughness [17], one can conclude that embrittlement results from toughness decrease rather than from a flaw build-up. The absence of microcracks is also indicative of a certain degree of homogeneity of oxidative degradation within fibre thickness. As a matter of fact, diffusion controlled oxidation would lead to a skin-core structure favouring microcracking due to the oxidation induced shrinkage in the skin [18].

In Fig. 5, strain at break is plotted in function of time of exposure. For 80 °C under 5 MPa $O_2$, strain at break values starting from 200% drop to 20% corresponding to a brittle behaviour after 60 h of exposure. For 110 °C in air, the ductile brittle transition occurs after 700 h of exposure. The ductile brittle transition time values (60 h against 700 h)

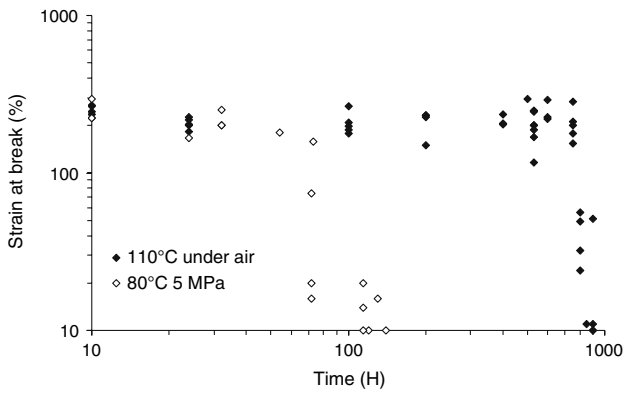


**Fig. 5** Strain at break as function of time of exposure: at 110 °C under air (♦) and at 80 °C under 5 MPa of oxygen (◇)

confirm that the first condition of exposure accelerates chain scission rate compared to the second one.

## Discussion

Two distinct exposure conditions have been studied. They lead to very different kinetic behaviours since induction times differ by about one order of magnitude. In both cases, $M_W$ decreases abruptly after the end of the induction period showing that oxidation induces predominant chain scission which in turn, induces chemicrystallization and fibre embrittlement. The first question which comes in mind is: Is it possible to establish a link between chemical parameters, for instance, the conversion ratio of the oxidation process and physical ones, for instance, the degree of embrittlement?

In amorphous glassy polymers, plasticity is obviously linked to chain drawing, the latter being only possible when chains are entangled. Embrittlement is thus expected to occur when entanglement network has been significantly degraded, i.e. when the molar mass reaches a critical value $M_C'$ higher than the rheological value $M_C$, but of the same order of magnitude [5]. The case of semi-crystalline polymers having their amorphous phase in rubbery state is more complicated because plasticity mechanisms are different [19, 20]. Is the concept of critical molar mass pertinent in this case? Various recent studies have shown that this concept is relevant to characterize ductile-brittle transition [8, 9], but the values of $M_C'$ are considerably higher than the entanglement molar mass $M_e$. In other words, embrittlement occurs while the entanglement network in the amorphous phase has undergone negligible degradation.

In order to check this result in the case under study, we have plotted the strain at break as a function of weight average molar mass for both exposure conditions in Fig. 6. Despite a noticeable scatter, two regimes separated by a sharp transition can be distinguished: the ductile regime with strain at break higher than 100% and the brittle regime with strain at break lower than 30%. The transition appears to be independent of exposure conditions within experimental scatter and located at $M_C' \sim 130$ kg mol$^{-1}$. This value is lower than for PP isotropic samples ($M_C' \sim 200$ kg mol$^{-1}$ [9]) but remains considerably higher than the entanglement molar mass ($M_e \sim 3.5$ kg mol$^{-1}$ [21]). It appears thus that the "embrittlement critical molar mass" is not only a polymer characteristic, but depends also on processing induced morphology, i.e. here macromolecular orientation. Indeed, whereas isotropic film is characterized by classical lamellae morphology, fibre morphology is characterized by a highly fibrillated structure [22, 23]. To check this

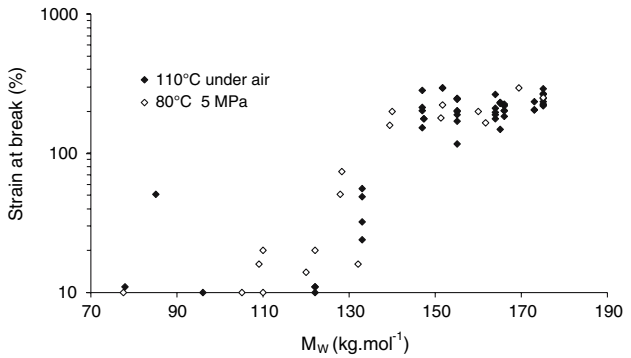


**Fig. 6** Strain at break as function of weight average molar mass ($M_W$) during exposure: at 110 °C under air (♦) and at 80 °C under 5 MPa of oxygen (◇)

orientation effect, the fibres were molten and compression moulded to obtain films. These latter displayed a brittle behaviour in tensile testing (strain at break ∼5%) which is not surprising since the weight average molar mass of fibres, 170 kg mol$^{-1}$, is lower than the critical molar mass for isotropic PP samples (200 kg mol$^{-1}$).

Since, during ageing, the entanglement network in the amorphous phase undergoes only minor changes, it seems logical to consider eventual effects of morphological changes. Our results put in evidence an increase of the crystallinity ratio due to annealing and chemicrystallization. In the case of isotropic samples, lamella thickening is observed [24, 25]. It is well known that highly crystalline polymers generally display a brittle behaviour and that small quantities of comonomers improve ductility by reducing crystallinity, in polyethylene as in polyoxymethylene, for instance. In the case of polyethylene, it has been clearly demonstrated that samples displaying an interlamellar distance lower than 6 nm are systematically brittle [10].

It seemed thus interesting to plot the strain at break against crystallinity ratio measured by WAXS in Fig. 7. Here, also, the points corresponding to both exposure conditions under study are close to a single curve displaying a sharp transition around $X_C \sim 80\%$. Since the chemiscrystallization process is expected to play an important role on polymer embrittlement, it seemed interesting to us to plot $X_C$ against $M_W$ in Fig. 8. As observed in the curves $X_C = f(\text{time})$ (Fig. 3), annealing and chemicrystallization are well decoupled in the case of exposure in air at 110 °C: annealing appears in Fig. 8 as a quasi-vertical process, whereas chemicrystallization is characterized by a pseudo-exponential dependence with a horizontal asymptote at $X_{C\infty} \sim 90\%$. The behaviour is more complex at 80 °C because, as previously quoted, degradation is so fast that chemicrystallization occurs before the end of annealing.

Despite the results' scattering, the curve obtained at 110 °C can be used to tentatively model chemicrystallization kinetics from the following hypotheses:

(i) At a given degraded state where the crystallinity ratio is $X_C$, one can define the "active" amorphous fraction as the amorphous fraction potentially able to crystallize. In theory, it would be $(1 - x_C)$, where $x_C = X_C/100$ is expressed in mass fraction, not in percentages. However, the existence of an asymptote at $X_{C\infty} = 90\%$ in Fig. 8 suggests that the samples under study cannot reach 100% crystallinity and that the active amorphous fraction is rather $(x_{C\infty} - x_C)$, where $x_{C\infty} = 0.9$.

(ii) The starting crystallinity ratio (just after annealing) is of the order of $x_{C0} = 0.65$.

(iii) The chemicrystallization yield is just proportional to the active amorphous fraction.

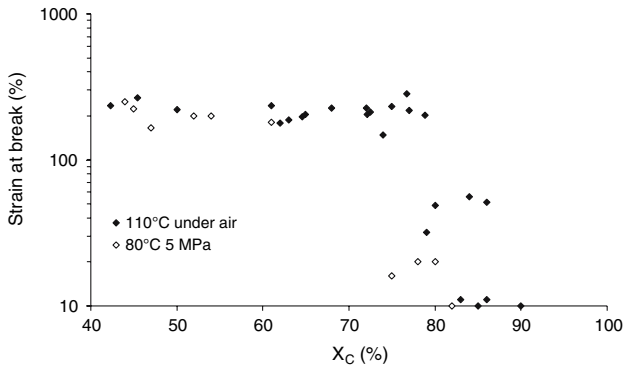


**Fig. 7** Strain at break as function of crystallinity ratio ($X_C$) during exposure: at 110 °C under air (♦) and at 80°C under 5 MPa of oxygen (◇)

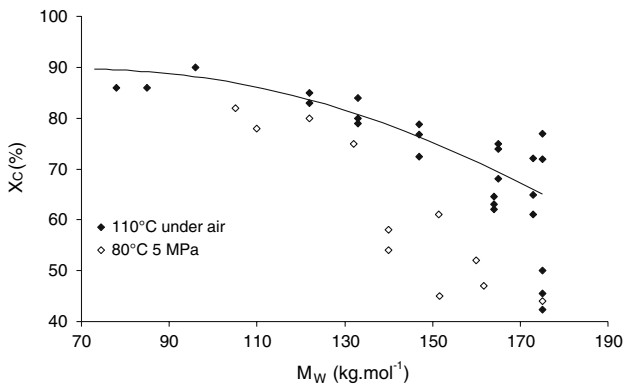


**Fig. 8** Crystallinity ratio ($X_C$) as function of weight average molar mass ($M_W$) during exposure: at 110 °C under air (♦), at 80 °C under 5 MPa of oxygen (◇) and modelling at 110 °C under air (solid curve)

$$\frac{dx_C}{ds} = A(x_{C\infty} - x_C)$$

Which gives:

$$x_C = x_{C\infty} - (x_{C\infty} - x_{C0})\exp(-As).$$

According to Fig. 8, one obtains:

$$x_C = 0.9 - 0.25\exp(-As)$$

with $A \sim 275$ kg mol$^{-1}$, $A$ would be almost temperature independent between 80 and 110 °C.

Just after annealing ($x_C \sim x_{C0} \sim 0.65$), it can be written:

$$\frac{\Delta x_C}{\Delta s} = 0.25A \approx 69 \text{ kg mol}^{-1}$$

Let us consider the case where $\Delta s = 1$ chain scission per initial weight average chain, which means that $M_W = 2/3M_{W0}$:

$$\Delta s = \frac{1}{M_{W0}}$$

Hence $\Delta x_C = \frac{69}{M_{W0}} = 0.4$

The number of methylenes entering the crystalline phase is thus:

$$\frac{0.4}{14 \times 10^{-3}} = 29 \text{ methylenes per kg or } \frac{29}{1/M_{W0}}$$
$$\approx 4,930 \text{ methylenes per chain scission}$$

Incidentally, in case where the process would be regarded only at the molecular scale, this state would correspond to a conversion ratio of $8 \times 10^{-5}$ bonds broken per initial chain bond. This result illustrates well the "amplifying effect" of structural scale changes: minor changes in molecular changes at the molecular scale can have big consequences at higher structural scales. Despite that, the chemicrystallization yield appears surprisingly high that can be tentatively explained as follows:

The average chain ends concentration $b$ is:

$$b = \frac{2}{M_n} = \frac{4.4}{M_W}$$

since the polydispersity index value is 2.2.

But crystallization rejects chain ends in the amorphous phase, so that:

$$b = \frac{4.4}{1 - x_{C0}} \frac{1}{M_W}$$

at the end of the annealing process.

In the same way, the average entanglement concentration $v$ is:

$$v = \frac{1}{2M_e},$$

where $M_e$ is the entanglement molar mass close to 3.5 kg mol$^{-1}$ for PP [21].

Since entanglements are also rejected in the amorphous phase, one has:

$$v = \frac{1}{2(1 - x_{C0})} \frac{1}{M_e}.$$

In fact, $v \leq \frac{1}{2(1-x_{C0})} \frac{1}{M_e}$ because orientation is known to disfavour entanglement.

The ratio number of chain ends per entanglement is thus:

$$\frac{b}{v} \geq \frac{8.8M_e}{M_W} = 0.18.$$

In other words, each chain scission occurs on an entanglement strand separated from a chain end by less than 5 entanglement junctions. This means that each chain scission can liberate many initially entangled chain segments allowing them to enter the crystalline phase. The process is favoured in highly oriented fibres by orientation of the amorphous phase.

## Conclusion

The oxidative degradation of polypropylene fibres for geotextile applications has been studied in two exposure conditions: 110°C in air at atmospheric pressure and 80 °C in pure oxygen at 5 MPa pressure corresponding to two ISO standards. Despite the lower temperature, the second method leads to induction period about 10 times lower than the first one, which corresponds to theoretical predictions.

Degradation has been monitored by rheometric molar mass determination, WAXS and tensile testing. Molar mass decreases suddenly after the end of the induction period, showing that random chain scission largely predominates. The molar mass drop is accompanied by a fast increase of crystallinity and a fast decrease of ductility. The embrittlement point corresponds to a molar mass of 130 kg mol$^{-1}$ and a crystallinity ratio of 80% whatever be the conditions of exposure. The causal chain can be ascribed:

(1) Chain scission in amorphous phase;
(2) Chain length reduction;
(3) Easier chain disentanglement;
(4) Chemicrystallization;
(5) Embrittlement.

Highly oriented fibres behave qualitatively in the same way as isotropic samples but with lower critical molar mass (130 against 200 kg mol$^{-1}$).

## References


1. Billingham NC, Calvert PD (1983) In: Allen NS (ed) Degradation and stabilisation of polyolefins. Applied Science Publishers, London, New York LDT, Chapter 1
2. Fayolle B, Audouin L, Verdu J (2000) Polym Deg Stab 70:333
3. Severini F, Gallo R, Ipsale S (1988) Polym Deg Stab 22:185
4. Kagiya T, Nishimoto S, Watanabe Y, Kato M (1985) Polym Deg Stab 12:261
5. Dai CA, Kramer EJ, Washiyama J, Hui CY (1996) Macromolecules 29:7536
6. Donald AM, Kramer EJ (1982) J Polym Sci Part B: Poly Phys 20:899
7. Creton C, Kramer EJ, Brown HR, Hui CY (2001) Adv Polym Sci 156:53
8. Fayolle B, Audouin L, Verdu J (2003) Polymer 44:2773
9. Fayolle B, Audouin L, Verdu J (2004) Polymer 45:4323
10. Fayolle B, Colin X, Audouin L, Verdu J (2007) Polym Deg Stab 92:231
11. Sen K, Kumar P (1995) J Appl Polym Sci 55:857
12. Kennedy MA, Peacock AJ, Mandelkern L (1994) Macromolecules 27:5297
13. Vink P, Fontijn HFN (2000) Geotextiles Geomembr 18:333
14. Richaud E, Farcas F, Bartoloméo P, Fayolle B, Audouin L, Verdu J (2006) Polym Deg Stab 91:398
15. Mead DW (1994) J Rheol 38:1797
16. Reich L, Stivala SS (1969) Autoxidation of hydrocarbons and polyolefins. Marcel Dekker, New York, p 475
17. Kausch HH, Heymans N, Plummer CJ, Decroly P (2001) Traité des matériaux, Matériaux polymers: propriétés mécaniques et physiques, Traité des Matériaux 14. Presses Polytecniques et Universitaires Romandes, p 376
18. Colin X, Mavel A, Marais C, Verdu J (2005) J Comp Mater 39:1371
19. Weynant E, Haudin JM, G'Sell C (1980) J Mater Sci 15:2677
20. Galeski A (2003) Prog Polym Sci 28:1643
21. Van Krevelen DW (1990) Properties of polymers, 3rd edn. Elsevier, Amterdam, p 465
22. Abo El-Maaty MI, Olley RH, Bassett DC (1999) J Mater Sci 34:1975
23. Risnes OK, Mather RR, Neville A, Buckman J (2003) J Mater Sci 38:2161
24. Zhang XC, Cameron RE (1999) J Appl Polym Sci 74:2234
25. Kostoski D, Stojanovic Z (1995) Polym Deg Stab 47:353